Terahertz Detection of Deoxyribonucleic Bases, Viruses and Nano Particles

Massood Tabib-Azar

Electrical and Computer Engineering Dept., University of Utah, Salt Lake City, USA

azar.m@utah.edu

***Abstract*— A metamaterial composed of diamond-shaped (70 μm X 35 μm) copper patches was designed and used to detect nanoparticles with 0.75-1.1 terahertz transmission spectroscopy. Deoxyribonucleic acid (DNA) bases adenine, thymine, cytosine, and guanine were detected and identified. Cytosine showed 1.7 dB higher absorption around 0.975 THz than the other bases. SARS-CoV-2 infected saliva showed different spectrum and -10 dB higher absorption than uninfected saliva over 0.75-1.1 THz. Other nanoparticles consisting of 100-500 nm antimony, carbon black, zeolite aluminosilicate molecular sieves), Terfenol-D ($Tb_{0.3}$ $Dy_{0.7}Fe_2$), Cu_2S, Ag_2S, dust collected from bench tops, 10-100 μm size diamond particles, red polystyrene beads, iron particles and graphene sheets were also tested. Sensor sensitivity for uninfected saliva was 0.3 dB/ng and for infected saliva was 0.8 dB/ng. The metamaterial surface studied here enables detection of airborne particles larger than 10 μm in diameter.**

Keywords—Biomarker, real-time viral sensors, Terahertz

I. INTRODUCTION

SARS-CoV-2 virus is known to resonantly absorb terahertz electromagnetic waves owing to the virus's vibrational modes [1]. The terahertz sensor discussed here has the potential to detect SARS-CoV-2 virus in 1-10 ms. Rapid (5-15 min) electronic SARS-CoV-2 sensors are reported [2-5] that usually require molecular recognition mechanisms based on aptamers or antibody/antigens for selective detection of viruses. Metamaterial (MTM) terahertz sensors do not require molecular recognition tags to differentiate between different particles. Viruses show different signature absorptions mostly in the 0.5-4 THz range in free space [1,6]. Our work reported here shows that coupling viruses and molecules with metallic focusing structures shifts their absorption peaks to lower frequencies making their detection more accessible with currently available commercial terahertz sources.

Our main objective is to develop a fast detection technique to sense airborne viruses. Preliminary studies by others have indicated that viruses such as SARS-CoV-2 absorb terahertz electromagnetic waves [1,6]. Label-free terahertz detection of SARS-CoV-2 can be enhanced by "focusing" structures such as bowtie antennas and by metamaterials. In addition to red-shifting absorptions, terahertz signals interacting with the MTM structures result in hotspots providing enhancements in detecting particles/viruses.

Here we use an MTM composed of 70 μm X 35 μm metallic diamond patches on a dielectric substrate (ε_r~3.8) (Fig. 1) to enhance electromagnetic interactions with airborne viral and other particles. SARS-CoV-2 become airborne and spread through aerosolized particulates generated by coughing or talking. Human saliva has an average relative permittivity of 76 [7], while water's relative permittivity is 80 at 20°C [8]. Saliva consists of 99 % water and 1-2 % of biomarkers, urea, ions, enzymes, and other vital components [9]. Saliva exhibits different electrical/dielectric characteristics in the same person depending on their hydration level, fasting, activity, age, and health conditions [10]. Saliva also contains viruses and bacteria in infected individuals. Viruses are composed of capsid proteins and glycoprotein and inner deoxyribonucleic acid (DNA) or ribonucleic acid (RNA) cores that determine their dielectric properties [11]. Most DNA and RNA viruses have dry relative dielectric constant of 8-10. Our main objective here is to develop terahertz virus sensors that take advantage of "focusing" resonant structures as well as resonant absorptions in viral particles to detect viruses sensitively and selectively.

The metamaterial used in this work consists of 70 μm x 35 μm diamond shape copper patches on a dielectric substrate (ε_r~3.8) that exhibit multiple resonances in the range of interest (0.75-1.1 THz).

The above metamaterial can be fabricated over large areas and can be interrogated using a terahertz beam. To the best of our knowledge the work reported here is the first description of a remote sensing technique capable of detecting SARS-CoV-2 viruses residing over large surfaces.

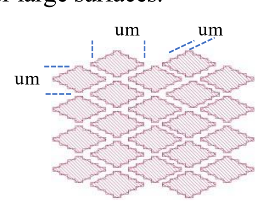

Fig. 1: Schematic of a diamond shaped metamaterial.

To detect low densities of materials including viruses, focusing structures are required. Metals used for focusing structures have large absorption coefficients in the terahertz range. Diamond patches used here are similar to partial mirrors developed for terahertz Fabry-Perot resonators reported before [12]. When virus-infected saliva particles (50 μm – 200 μm diameter) land on the meta surface sensors, they interact with the hot spot charges and change the transmission/reflection coefficients of the sensor surface. In surfaces without hot spots such as uniform dielectric substrates, the change in transmission/reflection coefficients is much smaller.

II. Experimental Procedure and Results

The experimental setup shown in Fig. 2 consists of a Keysight PNA N5224A and two Virginia Diode WR1.0 Extension modules covering 0.75-1.1 THz spectral range. The MTM sample we used in our measurement had diamond copper patches fabricated using a computer-controlled milling machine with 30 µm linewidth.

All powder and dry nanoparticle samples were deposited on a scotch tape without pressing. It is well-known that this method enables the scotch tape to pick up a very thin, nearly a molecular/single layer of powder material. Liquid samples (usually 1 µL) were deposited on the MTM and were subsequently supported by a thin film of dielectric (usually another layer of scotch tape) that resulted in a liquid film layer of ~ 20 µm thick held by surface forces. All the terahertz spectra had 1601 frequency points and were averaged over 50 nearby frequency points.

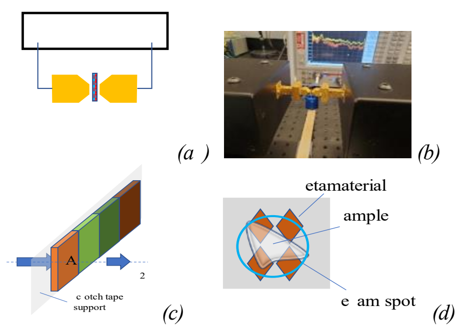

Fig. 2: a) Schematic of the terahertz spectroscopy system used in our work. Samples were located between the transceiver horns. b) Image of the setup. c) Samples deposited on a tape. d) Samples on a tape were pressed on the MTM. The THz beam was polarized along the diamond long axis.

DNA Bases: Detection and identification of DNA bases adenine (A), thymine (T), cytosine (C), and guanine (G) are of outmost importance in developing techniques to detect viruses. The DNA bases were deposited on scotch tape that picked up one molecular layer of the powder. They were then used directly to obtain the spectra shown in Fig. 3a. Subsequently, they were attached onto the MTM with the DNA side touching the copper patches. The MTM transmission spectra in this case is shown in Fig. 3b. All spectra were normalized to have the same magnitude at 0.75 THz. It is significant that even without the MTM, the DNA on scotch tape spectra are quite distinct. Theoretical and experimental studies in the past have shown that DNA bases have signature absorptions near 2 THz [13]. It appears that the scotch tape coated with DNA bases and the MTM have redshifted some of the absorption bands to below 1.1 THz. The spectra obtained with the MTM structure show enhancement of the absorption for the cytosine and has modified the other spectra as well. A near-field terahertz probe [14] may be able to differentiate between individual molecules of ATCG bases.

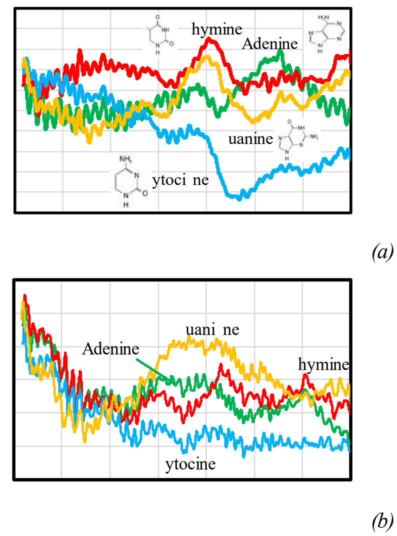

Fig. 3: Transmission spectra of a) DNA bases alone and b) DNA bases on the MTM structure.

SARS-CoV-2 and Uninfected Saliva Samples: We placed 1 µL of different saliva samples on the MTM and performed 3 consecutive measurements on each sample. A healthy person's saliva has a relative dielectric constant of 76 on average [7], and water has a relative dielectric constant of ~ 78-81 in room temperature depending on its ionic content. The infected saliva has -5 dB higher absorption at 0.75 THz and increased to -10 dB at 1.1 THz as shown in Fig. 4. There are other differences that will be explored in a future work.

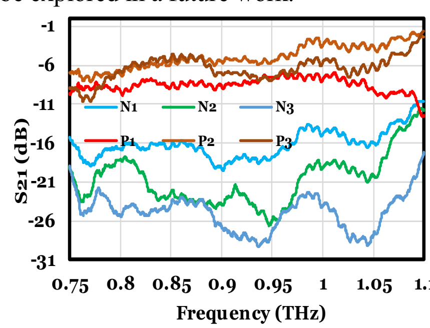

Fig. 4: Transmission spectra of the MTM with uninfected and SARS-CoV-2 infected saliva. Negative and Positive samples are denoted by "N" and "P", respectively.

The MTM structure improved the detection capability and identification of saliva by -5 dB compared to the uniform substrate. The selectivity of the terahertz technique in detecting SARS-CoV-2 is demonstrated in [1]. SARS-CoV-2 is negatively charged in the saliva and the combination of its structural response to terahertz signal along with its conductivity, and its interaction with the sharp metallic regions on the MTM, enhanced and contributed to its absorption spectrum shown in Fig. 4. Aptamers designed to bind with the spiking proteins of the SARS-CoV-2 [4] can be used to coat the MTM structure to increase its selectivity and specificity. The SARS-CoV-2 saliva samples used here were obtained from the University of Utah Medical School though a collaborative effort (please see the acknowledgement). A biosafety laboratory level 2 was used in the experiments.

Insulating/Semiconducting/Conducting Nanoparticles: Saliva particles may absorb other airborne materials such as dust, soot, rust/iron, silica, and other particles. Thus, it is important to understand the contribution of these particles in detection and identification of infected/uninfected saliva particles. To separate the inherent terahertz properties of these particles from the saliva and water, we present the experimental results using dry powders deposited on tapes.

Fig. 5a shows the results with diamond particles (few hundred micrometers in diameter), graphene flakes (up to 500 μm), and fine (~100 nm – 1 μm) dust particles. Diamond particles have the highest conductivity and scatter the terahertz signal the most resulting in the highest absorption beyond 0.8 THz. Dust particles, collected from benchtops, have the smallest absorption followed by the graphene flakes (50-100 μm dia.)

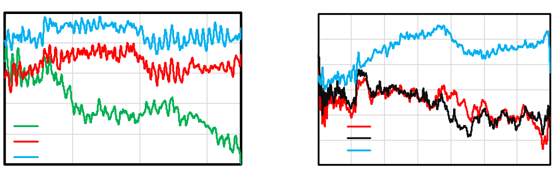

(a) *(b)*

Fig. 5: a) Transmission spectra of diamond, graphene and dust particles on the MTM. Dust particles are insulating compared to graphene. b) Transmission spectra of antimony, carbon black and zeolite particles on the MTM.

Fig. 5b shows the transmission spectra of antimony, carbon black and zeolite (aluminosilicate). Absorption in zeolite is smaller than antimony and carbon black. Zeolite is very insulating, and its particle size is around 1-10 μm according to our atomic force microscopy studies. Larger particle sizes can result in larger scattering rates and higher effective absorptions measured by the instrument as seen in diamond particles. Zeolite has a transmission window at 0.93 THz. Carbon black and antimony have "signature" spectral variations around 0.8 and 0.95 THz.

Fig. 6a shows transmission spectra of CuS_2, Ag_2S and $PdCl_2$ that are generally considered as memristor materials with large ionic conductivity components. Their absorption coefficients are similar to graphene, dust, antimony, carbon black, and zeolite. Notably, Cu_2O has a transmission window around 0.965 THz. $PdCl_2$ also has transmission peaks around 0.78 and 0.975 THz.

Next, we examined terahertz transmission spectra of polystyrene beads (10-100 μm dia. fluorescent), Terfenol-D and iron particles that are magnetic materials with high electrical conductivities, as shown in Fig. 6b. Polystyrene is a good insulator and has the smallest absorption coefficient followed by Terfenol-D and iron particles.

The above results can be analyzed using the relationship between the terahertz transmission coefficient (Γ_T) and the electromagnetic properties of the material: $\Gamma_T = 2Z_L/(Z_L+Z_s)$, where Z_L is the load impedance at the frequency of measurement and Z_s is the source impedance. The load impedance is the material impedance related to the material conductivity (σ), permittivity (ε) and permeability (μ): $Z_L = L/(A\sigma) + 1/(j\ \varepsilon A\omega/d)$ or: $Z_L = L/(A\sigma) + j\ \mu\ A^2/L$, where L is the sample length, and A is its cross-sectional area. L and A are related to the interaction volume with the terahertz beam. The terahertz wave is absorbed by the sample, transmitted, or scattered. Non-uniform samples consisting of particles with 10-100 μm sizes can strongly scatter the terahertz signals (1 THz wavelength is 300 μm). The transmitted power (P_t) is related to the total incident power (P_{in}), to the absorbed (P_a), reflected power (P_r) and scattered (P_{sc}) powers: $P_t = P_{in} - P_a - P_{sc} - P_r$. The transmitted and reflected powers are forward and back scattered powers and are routinely measured using simple experimental arrangements. P_{sc} contains important information regarding the particle size. P_a contains important information regarding absorption mechanisms in the sample. MTM contributes to all these components of the power and if not designed properly, it can increase the absorbed power significantly. It should have minimum absorption and scattering while creating intense hot spots to increase the electromagnetic interactions with the sample. In the transmission spectra shown in Figs. 3-8 conducting samples exhibited smaller transmission coefficients as expected since they have larger absorption coefficients.

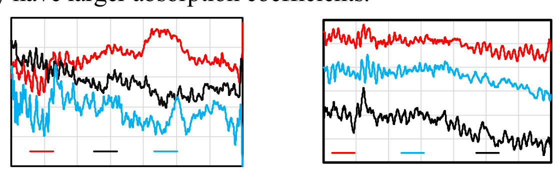

(a) *(b)*

Fig. 6: a) Transmission spectra of Cu_2O, Ag_2S and $PdCl_2$ on MTM. b) Transmission spectra of polyester red beads (10-120 μm in diameter), Terfenol-D powder, and iron particles (1-50 μm dia.).

The sensitivity of the terahertz technique is given by: $S_a = -\frac{\partial S_{21}}{\partial m}$, where S_{21} is the reflection coefficient and "m" is the material mass deposited on the senor. S_a for uninfected saliva was 0.3 dB/ng and for infected saliva was 0.8 dB/ng with MTM substrate at room temperatures.

III. Conclusion

We demonstrated the ability of a diamond-shaped MTM terahertz sensor in detecting and differentiating DNA bases, SARS-CoV-2 infected and uninfected saliva samples, and many conducting, semiconducting and insulating micro and nano-particles. All experimented particles were smaller than the THz wavelength (<λ/10) and were nearly one monolayer thick. The MTM increased the sensitivity of the terahertz technique across the board by more than -5 dB.

ACKNOWLEDGEMENT

This work was supported by a RAPID grant from NSF (#2030359), a grant from EXAMIN, LLC and by the USTAR Program. Infected saliva were obtained from Dr. Elizabeth Middleton of Department of Internal Medicine, University of Utah. SARS-CoV-2 sensors partially discussed here are being commercialized by the University of Utah.

REFERENCES

1. A. Ahmadivand, B. Gerislioglu, Z. Ramezani, A. Kaushik, P. Manickam, S. A. Ghoreishi, “Functionalized terahertz plasmonic metasensors: Femtomolar-level detection of SARS-CoV-2 spike proteins,” Biosensors and Bioelectronics, Volume 177, 2021, p. 112971, ISSN 0956-5663, https://doi.org/10.1016/j.bios.2021.112971.

2. Massood Tabib-Azar, Shaun McKellar, Cynthia Furse, “Free Space Resonant Electromagnetic Sensing Techniques to Detect Airborne Viral and Environmental Particles Using Atomic Layer Graphene.” NT21: International Conference on the Science and Application of Nanotubes and Low-Dimensional Materials. Proceeding, p. 65 (2021).

3. Massood Tabib-Azar, “Electronic Spiking Protein-Based COVID Sensors.” 2021 Meet. Abstr. MA2021-01 2036. https://iopscience.iop.org/article/10.1149/MA202101522036mtgabs/meta

4. Massood Tabib-Azar and Elizabeth Middleton, "Electronic Sensors to Detect COVID-19 Viruses in Real-Time." Accepted for publication in IEEE Sensors (6/202/2022).

5. R. I. MacCuspie, N. Nuraje, S. Y. Lee, A. Runge, and H. Matsui, “Comparison of electrical properties of viruses studied by AC capacitance scanning probe microscopy,” Journal of the American Chemical Society, vol. 130, no. 3. pp. 887–891, 2008, doi: 10.1021/ja075244z.

6. Soo Hyun Lee, Yeon Kyung Lee, Sang-Hun Lee, Jisung Kwak, Hyun Seok Song, Minah Seo, “Detection and discrimination of SARS-CoV-2 spike protein-derived peptides using THz metamaterials,” Biosensors and Bioelectronics, Vol. 202, 2022, p. 113981, ISSN 0956-5663, https://doi.org/10.1016/j.bios.2022.113981.

7. U. R. L. D. J. Shinde and S. C. Mehrotra, “Signal Processing as a Probe to Study Dielectric Properties of Mouth Cancer Patient’s Saliva,” vol. 4, no. 4, pp. 1483–1485, 2013.

8. J. L. Aragones, L. G. Macdowell, and C. Vega, “Dielectric Constant of Ices and Water: A Lesson about Water Interactions,” J. Phys. Chem. A, vol. 115, pp. 5745–5758, 2011, doi: 10.1021/jp105975c.

9. P. K. Dave, R. Rojas-Cessa, Z. Dong, and V. Umpaichitra, “Survey of saliva components and virus sensors for prevention of SARS-COV-2 and infectious diseases,” Biosensors, vol. 11, no. 1, 2021, doi: 10.3390/bios11010014.

10. M. Tabib-Azar and Nahid Antu, to be published.

11. R. I. MacCuspie, N. Nuraje, S. Y. Lee, A. Runge, and H. Matsui, “Comparison of electrical properties of viruses studied by AC capacitance scanning probe microscopy,” Journal of the American Chemical Society, vol. 130, no. 3. pp. 887–891, 2008, doi: 10.1021/ja075244z.

12. Li-Jin Chen, Tzeng-Fu Kao, Ja-Yu Lu, Chi-Kuang Sun, "A simple terahertz spectrometer based on a low-reflectivity Fabry-Perot interferometer using Fourier transform spectroscopy," Opt. Express 14, 3840-3846 (2006).

13. F Wang, D. Zhao, H. Dong, L. Jiang, Y. Liua, S. Li, “Terahertz spectra of DNA nucleobase crystals: A joint experimental and computational study,” Spectro Chimica Acta Part A: Molecular and Biomolecular Spectroscopy 179 (2017) 255–260.

14. O. Fawole and M. Tabib-Azar, "Terahertz quantification of ethanol and sugar concentrations in water and its application for noninvasive real-time monitoring of fermentation," in 2016 IEEE/MTT-S International Microwave Symposium (IMS), 22-27 May 2016, Piscataway, NJ, USA, 2016, p. 4 pp.

15. O. C. Fawole and M. Tabib-Azar, "Terahertz Near-Field Imaging of Biological Samples with Horn Antenna-Excited Probes," IEEE Sensors Journal, vol. 16, pp. 8752-60, 2016.